Oncogene (2006), 1–10

www.nature.com/onc

ORIGINAL ARTICLE

Reduction of apoptosis in *Rb*-deficient embryos via *Abl* knockout

HL Borges[1], IC Hunton and JYJ Wang

Division of Hematology/Oncology, Department of Medicine, Moores Cancer Center, School of Medicine, University of California San Diego, La Jolla, CA, USA

The retinoblastoma protein RB regulates cell proliferation, differentiation and apoptosis. Homozygous knockout of *Rb* in mice causes embryonic lethality owing to placental defects that result in excessive apoptosis. RB binds to a number of cellular proteins including the nuclear Abl protein and inhibits its tyrosine kinase activity. *Ex vivo* experiments have shown that genotoxic or inflammatory stress can activate Abl kinase to stimulate apoptosis. Employing the *Rb*-null embryos as an *in vivo* model of apoptosis, we have shown that the genetic ablation of *Abl* can reduce apoptosis in the developing central nervous system and the embryonic liver. These results are consistent with the inhibitory interaction between RB and Abl, and provide *in vivo* evidence for the proapoptotic function of Abl.
Oncogene advance online publication, 18 December 2006; doi:10.1038/sj.onc.1210157

Keywords: central nervous system; fetal live; haploid insufficiency; knockout mice; tumor suppressor

Introduction

The human retinoblastoma susceptibility gene, *Rb*, encodes a nuclear protein that regulates cell cycle progression, terminal differentiation and programmed cell death (Chau and Wang, 2003; Liu *et al*., 2004; Nguyen and McCance, 2005). In mice, the constitutive knockout of *Rb* causes embryonic lethality resulting from defects in placental function (Clarke *et al*., 1992; Jacks *et al*., 1992; Lee *et al*., 1992; de Bruin *et al*., 2003; Wu *et al*., 2003). The *Rb*-knockout embryos exhibit inappropriate cell cycle entry and massive apoptosis in the developing central nervous system (CNS), peripheral nervous system, lens, liver and muscles (Clarke *et al*., 1992; Jacks *et al*., 1992; Lee *et al*., 1992). The excessive apoptosis, but not the ectopic S-phase, of *Rb*-null embryos is rescued when the embryos are developed on wild-type placentas (de Bruin *et al*., 2003; Wu *et al*., 2003).

The mechanism by which RB inhibits cell proliferation is well established. RB interacts with E2F to repress transcription of genes critical for cell cycle progression (Liu *et al*., 2004; Nguyen and McCance, 2005). The ectopic cell proliferation in *Rb*-null embryos is suppressed by the knockout of *E2f1* or *E2f3*, providing *in vivo* evidence for the critical role of RB in the control of E2F activity (Tsai *et al*., 1998; Ziebold *et al*., 2001). The *E2f*-knockouts also reduced the apoptosis of *Rb*-null embryos, consistent with the proapoptotic functions of E2F (Tsai *et al*., 1998; Ziebold *et al*., 2001). Overproduction of E2F-1 in combination with the deprivation of survival signals can lead to activation of p53-dependent apoptosis through the intrinsic death pathway (Hickman *et al*., 2002; Sherr and McCormick, 2002). Consistently, the knockout of *p53* or *Apaf-1* also reduced apoptosis in the *Rb*-null embryos (Morgenbesser *et al*., 1994; Macleod *et al*., 1996; Guo *et al*., 2001). These results suggest the *Rb*-null placental defects can somehow activate the intrinsic apoptotic pathway in the *Rb*-null embryos. In cultured cells, E2F-1 upregulates the expression of p19Arf, which activates p53 through the sequestration of Mdm2 (Hickman *et al*., 2002; Sherr and McCormick, 2002). However, knockout of p19Arf did not rescue the apoptotic phenotype of *Rb*-null embryos (Tsai *et al*., 2002). This result suggests that p53 maybe activated by other pathways to induce apoptosis in the *Rb*-null embryos.

The RB protein contains several distinct peptide-binding 'pockets' that mediate its interaction with a large number of viral and cellular proteins (Morris and Dyson, 2001; Chau and Wang, 2003). The interaction between RB and the C-terminal peptide of E2F-1, E2F-2 and E2F-3 has been elucidated by X-ray crystallography to involve the RB A/B domain (Lee *et al*., 2002; Xiao *et al*., 2003). The crystal structure of a shallow groove in the RB B-domain binding to the LxCxE-peptide found in viral oncoproteins such as E7 has also been solved (Lee *et al*., 1998; Liu *et al*., 2006). Recently, the three-dimensional structure of RB C-region in complex with an E2F/DP heterodimer has been reported (Rubin *et al*., 2005). The RB C-region also interacts with a Pro, Glu, Asn, Phe ('PENF') peptide motif found in several cellular proteins (Darnell *et al*., 2003), and a binding site for cyclin-dependent protein kinases (Adams *et al*., 1999). A majority of the RB-interacting proteins are

Correspondence: Dr JYJ Wang, Moores Cancer Center, Room 4328, School of Medicine, University of California, San Diego, 3855 Health Sciences Drive, La Jolla, CA 92093-0820, USA.
E-mail: jywang@ucsd.edu
[1]Current address: Instituto de Ciências Biomédicas, Departamento de Anatomia, Universidade Federal do Rio de Janeiro, Centro de Ciências da Saúde, Rio de Janeiro, 21.941-590, Brazil.
Received 16 August 2006; revised 13 October 2006; accepted 17 October 2006

regulators of transcription (Morris and Dyson, 2001). By simultaneous binding multiple proteins, RB can assemble specific promoter complexes to regulate gene expression, and thus control cell proliferation, differentiation and apoptosis (Morris and Dyson, 2001; Hickman *et al*., 2002; Sherr and McCormick, 2002; Chau and Wang, 2003; Liu *et al*., 2004; Nguyen and McCance, 2005).

We have previously shown that the C-region of RB can bind to the Abl tyrosine kinase, leading to the inhibition of kinase activity (Welch and Wang, 1993,1995). Subsequent studies of RB C-region binding partners have led to the identification of a 'PENF' motif that is present in Abl, cPLA2, BRCA1, and several other cellular proteins as the motif recognized by the RB 'C-pocket' (Darnell *et al*., 2003). The 'PENF' motif is present in the Abl kinase domain, at the C-helix of the kinase N-lobe. Recent crystal structures have demonstrated the orientation of the Abl C-helix to play a critical role in the regulation of Abl activity (Levinson *et al*., 2006) supporting the conclusion that RB binding to the Abl C-helix causes an inhibition of the tyrosine kinase activity (Welch and Wang, 1993, 1995).

Abl is activated by genotoxins and tumor necrosis factor (TNF) to stimulate apoptosis (Agami *et al*., 1999; Gong *et al*., 1999; Yuan *et al*., 1999; Wang, 2000; Chau *et al*., 2004). Abl is also activated during amyloid-β-peptide induced neuronal cell death (Alvarez *et al*., 2004). The oncogenic BCR-ABL of chronic myelogenous leukemia (CML) can stimulate cell death when it is trapped in the nucleus of CML cells (Vigneri and Wang, 2001; Aloisi *et al*., 2006). The Abl tyrosine kinase can activate the apoptotic function of p53 and p73 (Agami *et al*., 1999; Gong *et al*., 1999; Sionov *et al*., 1999; Yuan *et al*., 1999; Goldberg *et al*., 2002; Vella *et al*., 2003). Therefore, we tested whether Abl might play a role in the apoptotic phenotype of the *Rb*-null embryos.

The *Abl*-null mice exhibit neonatal lethality with an array of developmental defects including lymphopenia and osteoporosis (Tybulewicz *et al*., 1991; Li *et al*., 2000). In this study, we combined the *Abl*-null allele with the *Rb*-null allele and found that the loss of *Abl* could rescue apoptosis in a subset of *Rb*-null tissues between embryonic days E11–E13.

Results

Abl-*heterozygosity delayed the death of* Rb-*null embryos*

The $Abl^{+/-}$ (Tybulewicz *et al*., 1991) and $Rb^{+/-}$ mice (Jacks *et al*., 1992) in the 129/sv inbred genetic background were intercrossed to generate compound heterozygous $Rb^{+/-}Abl^{+/-}$ mice. We did not find any pups with the $Rb^{-/-}$ genotype from mating of the compound heterozygous mice; thus, *Abl*-knockout did not rescue the lethality of *Rb*-null embryos. We conducted a large-scale mating, collected a total of 1029 embryos between E10 and E14.5, determined their genotypes and assessed their viability (Figure 1). The allele frequency segregated by embryonic days is summarized in Figure 1a. The numbers of embryos collected at E10–E10.5 ($n=83$) and E14–E14.5 ($n=78$) were not sufficient to obtain a reliable distribution of nine genotypes. We therefore determined the allele frequency among the 1029 embryos (E10–E14.5) and found the nine genotypes to occur according to the Mendelian ratio (Figure 1b), suggesting a minimum loss of dead embryos by resorption between E10 and E14.5. We then analysed the percentage of dead embryos for each genotype between E10 and E14.5 (Figure 1c). Death of the $Rb^{-/-}Abl^{+/+}$ embryos occurred from E12 through E14.5, consistent with previous reports (Clarke *et al*., 1992; Jacks *et al*., 1992; Lee *et al*., 1992; de Bruin *et al*., 2003; Wu *et al*., 2003). We found a statistically significant reduction ($P<0.05$) of death with the $Rb^{-/-}Abl^{+/-}$ embryos when compared to $Rb^{-/-}Abl^{+/+}$ embryos (Figure 1c). By contrast, the $Rb^{-/-}Abl^{-/-}$ genotype did not prolong embryo survival between E12 and E13.5 (Figure 1c). With the 78 embryos collected between E14–E14.5, only one was of the $Rb^{-/-}Abl^{-/-}$ genotype. Although that one embryo was alive (Figure 1c), the frequency of $Rb^{-/-}Abl^{-/-}$ genotype was much lower than the Mendelian ratio during E14–E14.5 (Figure 1a). The knockout of *Abl* has been shown to cause late embryonic or neonatal lethality in mice (Tybulewicz *et al*., 1991). In this study, we also observed a low level (10–20%) of dead embryos with the $Rb^{+/+}Abl^{-/-}$ and $Rb^{+/-}Abl^{-/-}$ genotypes between E13 and E14.5 (Figure 1c). Taken together, these analyses show that the loss of one *Abl* allele, but not the complete ablation of *Abl*, could delay the death of *Rb*-null embryos.

$Rb^{-/-}$ *erythrocyte differentiation defect not corrected by* Abl *knockout*

Rb-deficient embryos exhibit defects in erythropoiesis (Clarke *et al*., 1992; Jacks *et al*., 1992; Lee *et al*., 1992). During mouse development, nucleated red blood cells derived from the yolk sac are found in embryonic circulation up to E11.5. Mature erythrocytes (enucleated) derived from the embryonic liver start to appear in the circulation around E12. In the $Rb^{-/-}$ embryos, development of enucleated mature erythrocytes is blocked. We examined blood smears from $Rb^{+/+}Abl^{+/+}$ as well as $Rb^{-/-}Abl^{+/+}$, $Rb^{-/-}Abl^{+/-}$ and $Rb^{-/-}Abl^{-/-}$ embryos at E12.5 and E13.5 to determine the effect of *Abl* loss on erythroid differentiation (Figure 2). At E12.5, blood smears showed $\sim$80% of nucleated erythrocytes in embryos of all genotypes examined. At E13.5, the percentage of nucleated erythrocytes was 49% in the blood smears of $Rb^{+/+}Abl^{+/+}$ embryos, but the level remained close to 80% in $Rb^{-/-}$ embryos irrespective of *Abl* genotypes (Figure 2). This result shows that *Abl* does not play a role in the erythroid developmental defect of $Rb^{-/-}$ embryos.

Effect of Abl *on apoptosis in the developing nervous system of* Rb-*null embryos*

The peripheral nervous system (PNS) of $Rb^{-/-}$ embryos undergoes caspase-3 dependent apoptosis, which is

a

Genotype / Embryonic Days	$Rb^{+/+}$			$Rb^{+/-}$			$Rb^{-/-}$		
	$Abl^{+/+}$	$Abl^{+/-}$	$Abl^{-/-}$	$Abl^{+/+}$	$Abl^{+/-}$	$Abl^{-/-}$	$Abl^{+/+}$	$Abl^{+/-}$	$Abl^{-/-}$
E10~10.5 (n=83)	4.8	18.1	4.8	10.8	24.1	10.8	6	18.7	2.4
E11~11.5 (n=342)	7.0	11.1	6.4	13.7	25.2	12.3	6.4	11.1	6.7
E12~12.5 (n=267)	6.7	13.1	7.1	13.9	19.5	14.6	5.2	13.1	6.7
E13~13.5 (n=259)	7	14.7	6.6	12.4	25.9	11.6	4.6	14	4.3
E14~14.5 (n=78)	2.6	18	7.7	16.7	25.6	7.7	2.6	18	1.3
Observed frequency (%) / Expected frequency (%)	6.25	12.5	6.25	12.5	25	12.5	6.25	12.5	6.25

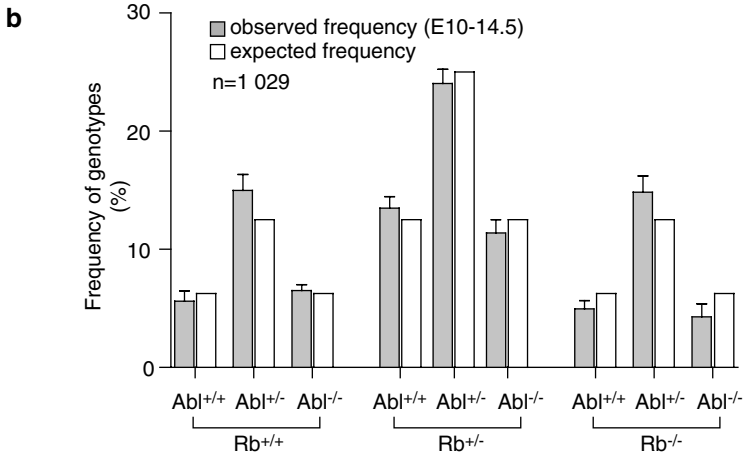

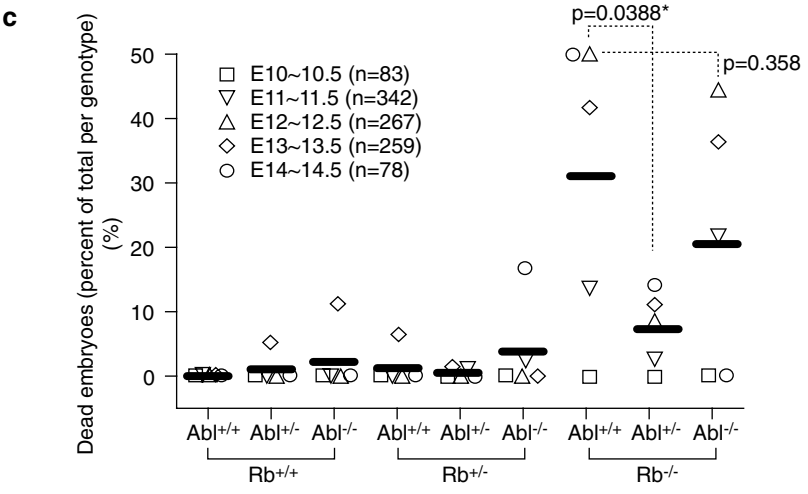

Figure 1 Genotypic distribution and embryonic death rate in the crosses among mice heterozygous for *Abl* and *Rb* genes. (**a**) The percentages of embryos per genotype on the indicated embryonic days as compared with expected frequency from Mendelian distribution. The embryos (total number under study denoted with *n*) from the crosses were genotyped on a given embryonic day. The observed frequency of embryos of a given genotype was tabulated as percent of the total number of embryos examined. (**b**) The percentages of embryos per genotype as compared with expected frequency from Mendelian distribution during the time span between embryonic days 10–14.5. The observed frequency of embryos for a given genotype is expressed as percentages of the total number of embryos examined ($n = 1029$). The corresponding expected frequency from Mendelian distribution is plotted alongside for comparison. No significant difference exists between the observed and the expected frequencies as determined by unpaired *t*-test ($P > 0.05$). (**c**) The frequency of embryonic death per genotype. The percentage of death embryos for a given genotype among the total number of embryos examined on a given embryonic day is plotted as the function of genotype, with different geometric symbols corresponding to the data collected on various embryonic days. The total number of embryos examined on a given day is denoted with *n* in parenthesis. The embryonic death rate associated with the genotype of $Rb^{-/-}Abl^{+/+}$ is significantly greater than that of $Rb^{-/-}Abl^{+/-}$ as determined by paired *t*-test ($P = 0.0388$).

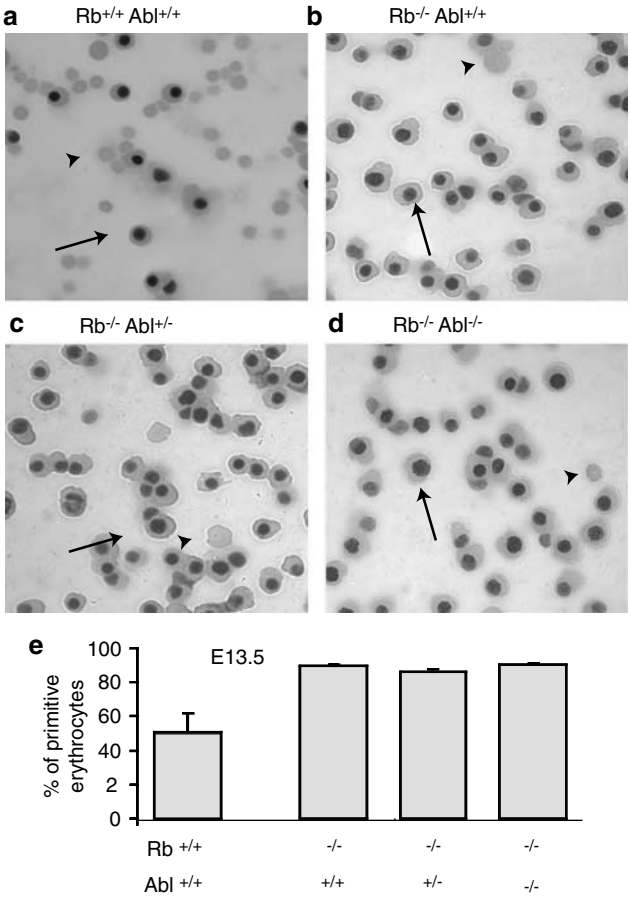

Figure 2 *Rb*$^{-/-}$ defect on erythrocyte differentiation not affected by *Abl* deletion. (**a**–**d**) Photomicrographs of peripheral blood stained with Wright–Giemsa with the indicated genotype at E13.5. Arrows show primitive erythrocytes nucleated, and arrowhead definitive erythrocytes enucleated. (**e**) Histogram shows the percentage of primitive erythrocytes with the indicated genotypes.

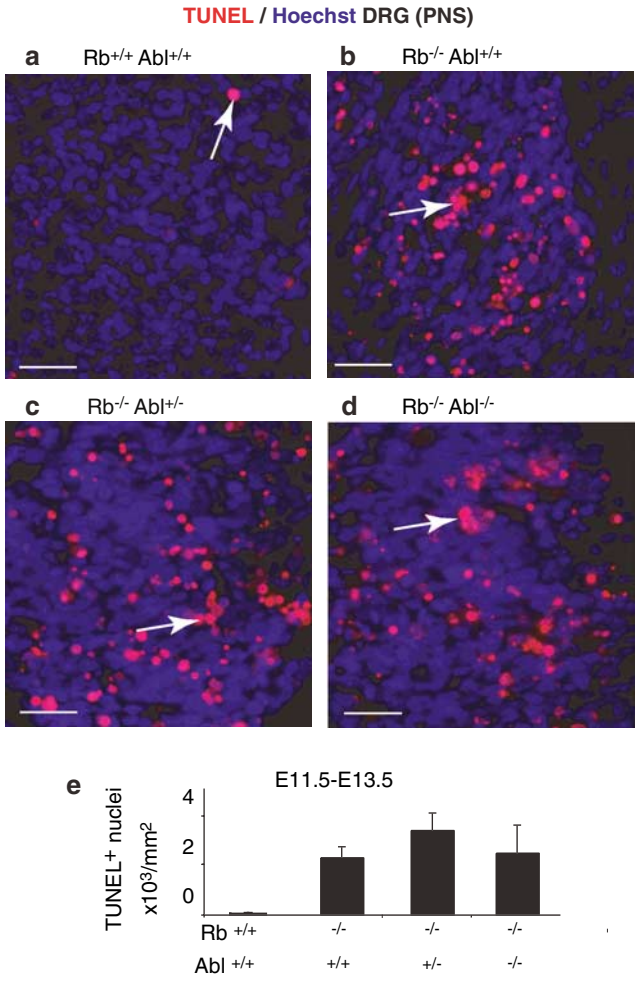

Figure 3 Apoptosis in peripheral nervous system not affected by *Abl* deletion. (**a**–**d**) Photomicrographs of E11.5 DRG sections stained with bisbenzimide (Hoechst-blue) and processed for TUNEL assay (red) with the indicated genotypes. Arrows indicate TUNEL-positive nuclei. Scale bar = 50 μm. (**e**) Histogram shows the number of TUNEL-positive nuclei and s.e.m. in the dorsal roof ganglia from E11.5 to E13.5 embryos with the indicated genotypes. The differences in the number of TUNEL positive nuclei were statistically insignificant (Dunnett's test $P > 0.05$) among the three genotypes *Rb*$^{-/-}$*Abl*$^{+/-}$ and *Rb*$^{-/-}$*Abl*$^{-/-}$ with *Rb*$^{-/-}$*Abl*$^{+/+}$.

readily detected in the sensorial ganglia (Clarke *et al*., 1992; Jacks *et al*., 1992; Lee *et al*., 1992). To investigate whether *Abl* is necessary for apoptosis in the developing PNS, sagittal sections of E11.5–E13.5 embryos were processed for TdT-mediated dUTP nick end labeling (TUNEL) assay. As expected, the number of TUNEL-positive nuclei in the dorsal root ganglia (DRG) was low in the *Rb*$^{+/+}$*Abl*$^{+/+}$ embryos (Figure 3a) and abnormally high in the *Rb*$^{-/-}$*Abl*$^{+/+}$ embryos (Figure 3b). The levels of TUNEL-positive nuclei in the DRG remained high in *Rb*$^{-/-}$*Abl*$^{+/-}$ and *Rb*$^{-/-}$*Abl*$^{-/-}$ embryos (Figure 3c and d). The different enumerations of TUNEL-positive nuclei in *Rb*$^{-/-}$ embryos were statistically insignificant among the three *Abl* genotypes (Figure 3e). Thus, *Abl* is not required for the ectopic cell death in the developing *Rb*$^{-/-}$ PNS.

The developing CNS of *Rb*$^{-/-}$ embryos exhibits increased apoptosis that is reduced by the knockout of *E2f-1*, *E2f-3*, *p53* or *Apaf-1* (Morgenbesser *et al*., 1994; Macleod *et al*., 1996; Tsai *et al*., 1998; Guo *et al*., 2001; Ziebold *et al*., 2001; Chau and Wang, 2003). The abnormal apoptosis is especially intense in the intermediate zone of the hindbrain (Figure 4b). We found that the knockout of *Abl*, either one or both alleles, can reduce the CNS apoptosis in a subset of *Rb*-null embryos, which we denoted as the Type 1 embryos (reduced apoptosis; Figure 4c and d). However, in another subset of *Rb*-null embryos that we denoted as Type 2, the knockout of *Abl* exerted no protective effect (excessive apoptosis; Figure 4e and f). Quantification of TUNEL-positive nuclei showed a statistically significant reduction of apoptosis in the Type 1 *Rb*$^{-/-}$ embryos of either *Abl*$^{+/-}$ or *Abl*$^{-/-}$ genotype (Figure 4g). The underlying cause for the phenotypic variation between the Type 1 and 2 embryos is unclear; however, we observed an embryonic age-dependence in their occurrence. At E11.5, we found three *Rb*$^{-/-}$*Abl*$^{+/-}$ embryos out of five (60%) and four *Rb*$^{-/-}$*Abl*$^{-/-}$ embryos out of

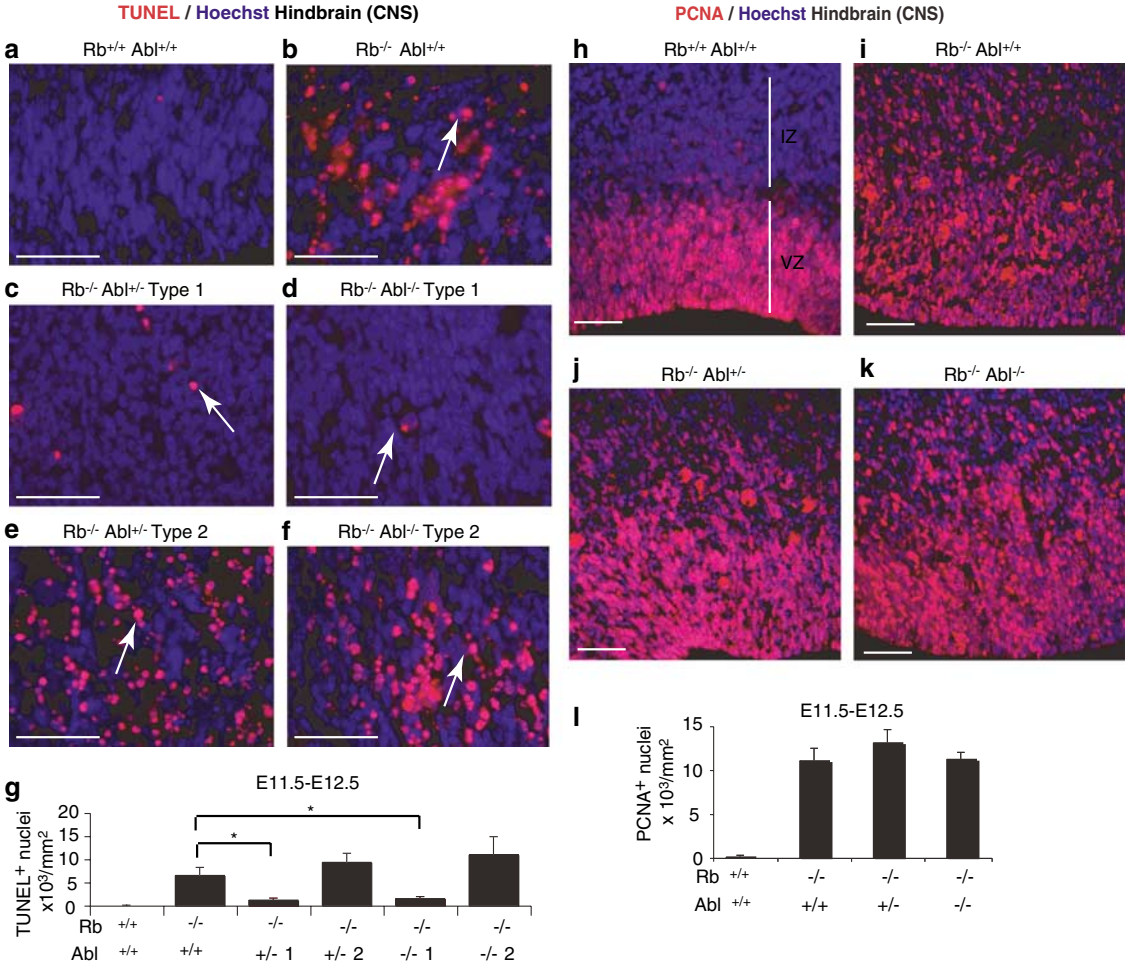

Figure 4 Loss of Abl attenuated CNS apoptosis but not ectopic proliferation in $Rb^{-/-}$. (**a**–**f**) Photomicrographs of sagittal sections of E11.5 hindbrain processed for TUNEL assay (red) counterstained with bisbenzimide (Hoechst-blue) and with the indicated genotypes. Arrows indicate TUNEL-positive nuclei. (**g**) Histogram shows the average number of TUNEL-positive nuclei and s.e.m. at the hindbrain from E11.5 to E12.5 embryos with the indicated genotypes ($P<0.05$ Dunnett's test comparing $Rb^{-/-}Abl^{+/-}$ and $Rb^{-/-}Abl^{-/-}$ with $Rb^{-/-}Abl^{+/+}$). (**h**–**k**) Photomicrographs of sagittal sections of hindbrain stained for PCNA immunohistochemistry (red) and counterstained with bisbenzimide (Hoechst-blue) with the indicated genotypes. VZ, ventricular zone; IZ, intermediated zone. (**l**) Histogram shows the mean number of PCNA-positive cells and s.e.m. at the hindbrain from E11.5 to E12.5 embryos with the indicated genotypes. Scale bar = 50 μm.

seven (57%) to be of Type 1. At E12.5, we found one $Rb^{-/-}Abl^{+/-}$ embryos out of five (20%) and one $Rb^{-/-}Abl^{-/-}$ embryos out of four (25%) to exhibit the Type 1 phenotype. At E13 and beyond, all of the $Rb^{-/-}$ embryos exhibited the Type 2 phenotype, that is, undergoing CNS apoptosis, irrespective of their *Abl* genotype. These results show that the loss of one *Abl* allele is sufficient to reduce the ectopic apoptosis of the developing CNS in the *Rb*-null embryos but the protective effect of *Abl*-loss was limited to early embryos.

Besides increased apoptosis, ectopic proliferation is also observed in the CNS of $Rb^{-/-}$ embryos (Clarke *et al*., 1992; Jacks *et al*., 1992; Lee *et al*., 1992). As discussed in the Introduction, the CNS apoptosis and proliferation phenotypes of *Rb*-null embryos are differentially rescued by the wild-type placentas (de Bruin *et al*., 2003; Wu *et al*., 2003). We assessed the ectopic CNS proliferation by staining sections from E11.5 to E13.5 embryos for the expression of proliferating cell nuclear antigen (PCNA) (Figure 4h–k). We found similar levels of PCNA-positive nuclei in the intermediate zone of $Rb^{-/-}Abl^{+/-}$ and $Rb^{-/-}Abl^{-/-}$ embryos irrespective of their apoptosis phenotypes. In other words, similar levels of PCNA-positive nuclei were detected in embryos with the Type 1 and the Type 2 apoptosis phenotypes. Therefore, we found no association between ectopic proliferation and apoptosis in the CNS, nor did we detect any effect of the *Abl* genotype on the number of PCNA-positive cells (Figure 4h–k). We also injected the pregnant mother with 5-bromodeoxyuridine (BrdU) 1 h before the harvesting of E13.5 embryos and examined DNA synthesis in the CNS (Figure 5a–d). Similar to the PCNA-staining result, ectopic proliferation was detected in the intermediate zone of the $Rb^{-/-}$ CNS, but this phenotype was not affected by the *Abl* genotype (Figure 5b–d and f). Taken

together, results in Figures 4 and 5 show that the reduction of CNS apoptosis in *Rb*-null embryos through *Abl* deficiency is limited to early embryonic days and independent of ectopic proliferation.

Loss of Abl *attenuated cell death in* $Rb^{-/-}$ *embryonic liver*

Increased apoptosis and decreased cellularity have been previously observed in the liver of *Rb*-null embryos (Clarke *et al*., 1992; Jacks *et al*., 1992; Lee *et al*., 1992; Zacksenhaus *et al*., 1996). To investigate whether *Abl* contributes to this phenotype of *Rb*-null embryos, sagittal sections of livers from E11.5 to E13.5 embryos were processed for TUNEL assay. The number of TUNEL-positive nuclei was significantly higher in the $Rb^{-/-}Abl^{+/+}$ liver (Figure 6b and e) than the $Rb^{+/+}$ $Abl^{+/+}$ liver (Figure 6a and e), confirming the previous finding of embryonic liver apoptosis that is also caused by the *Rb*-null placental defect (de Bruin *et al*., 2003; Wu *et al*., 2003). We observed a reduction in the liver apoptotic phenotype with the introduction of one *Abl*-null allele (Figure 6c and e). The complete loss of *Abl* further decreased cell death in the liver of *Rb*-null embryos (Figure 6d and e). The protection from apoptosis mediated by the loss of *Abl* in the embryonic

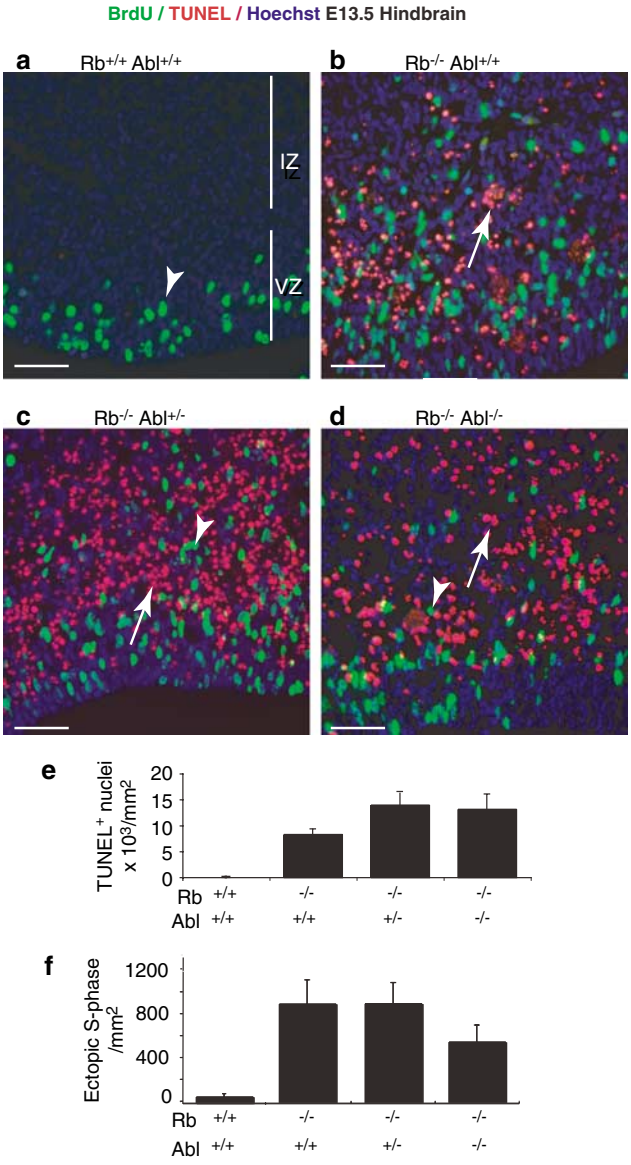

Figure 5 CNS apoptosis attenuation by Abl loss in the $Rb^{-/-}$ is embryonic day limited. (**a**–**d**) Photomicrographs of sagittal sections of E13.5 hindbrain processed for TUNEL assay (red) and IHC for BrdU (green), sections were also counterstained with bisbenzimide (Hoechst-blue). Genotypes are indicated above each photomicrograph. Arrows indicate TUNEL-positive nuclei and arrowheads indicate BrdU-positive nuclei. VZ, ventricular zone, IZ, intermediated zone. (**e**, **f**) Histograms show the average number of TUNEL-positive nuclei (**e**), BrdU-positive nuclei (**f**) and s.e.m. at the hindbrain from E13.5 embryos with the indicated genotypes. Scale bar = 50 μm ($P<0.05$ for both histograms, Dunnett's test comparing $Rb^{-/-}Abl^{+/-}$ and $Rb^{-/-}Abl^{-/-}$ with $Rb^{-/-}Abl^{+/+}$).

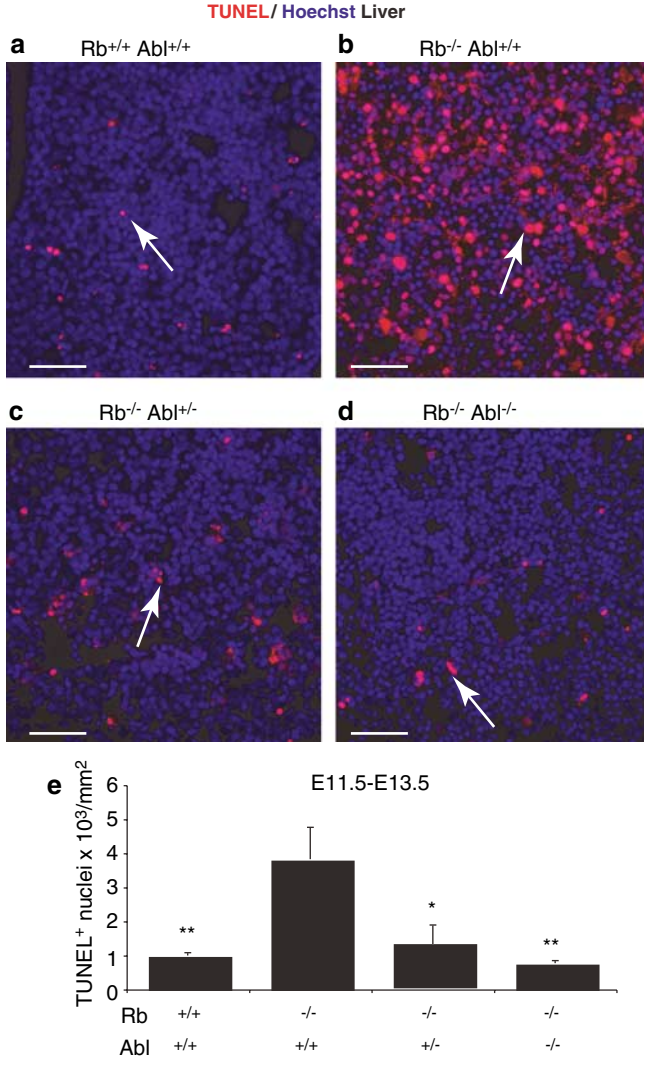

Figure 6 Loss of Abl decreased cell death in $Rb^{-/-}$ liver. (**a**–**d**) Photomicrographs of liver sections processed for TUNEL assay (red) and counterstained with bisbenzimide (Hoechst-blue), with the indicated genotypes from E13.5 embryos. Arrows indicate TUNEL-positive nuclei. (**e**) Histogram shows the mean number and s.e.m. of TUNEL-positive nuclei from E11.5 to E13.5 embryos with the indicated genotypes. Scale bar = 50 μm (*$P<0.05$, **$P<0.01$ in Dunnett's test comparing the data from indicated genotypes with that of $Rb^{-/-}Abl^{+/+}$).

liver was consistently observed in embryos from E11.5 through E13.5 without exception.

Discussion

Results from this study provide the first *in vivo* evidence for the proapoptotic function of Abl. Previous studies have demonstrated the proapoptotic function of Abl in cultured cell lines or explanted thymocytes (Agami *et al*., 1999; Gong *et al*., 1999; Yuan *et al*., 1999; Wang, 2000; Chau *et al*., 2004). With the *Rb*-null embryos as an *in vivo* model of apoptosis, we have shown *Abl* to play a role in the apoptosis of embryonic tissues.

The excessive apoptosis of *Rb*-null embryos is caused by defects in the placenta because $Rb^{+/+}$ placenta completely rescued the apoptotic phenotype of $Rb^{-/-}$ embryos (de Bruin *et al*., 2003; Wu *et al*., 2003). While it is clear that apoptosis is the result of placental defects, the actual trigger of death in the developing *Rb*-null embryos may be variable. Previous studies and the present report have shown that apoptosis of $Rb^{-/-}$ embryos is partially reduced by the knockout of *Caspase-3*, *Apaf-1*, *p53*, *E2f-1*, *E2f-3* or *Abl* (Table 1). Each of these gene knockouts exhibited a diverse spectrum of antiapoptotic effects (Table 1), suggesting different pathways may be activated in distinct embryonic tissues to cause death. Furthermore, our result suggests that the developmental age may also affect the mechanism of CNS apoptosis in *Rb*-null embryos.

We have found *Abl* to be required for the *Rb*-null CNS apoptosis in 50–60% of the E11 embryos, 20–25% of the E12 embryos but not in the E13 embryos. Between E11 and E13, the embryos undergo rapid growth and become dependent on mature erythrocytes (RBC) for oxygen (Kaufman, 1992). Embryo-intrinsic developmental programs and embryo-extrinsic factors, such as the number of embryos in the litter, determine the kinetics of embryo growth and the switching to RBC. Therefore, phenotypic variations among E11–E13 embryos are not unexpected. We have found that the knockout of *Abl* did not correct the erythroid differentiation defect. A previous report has suggested that hypoxia caused by the erythroid differentiation defect contributed to the CNS apoptosis in *Rb*-null embryos (MacPherson *et al*., 2003). It is thus possible that the Type 2 embryos, in which CNS apoptosis is not abrogated by *Abl* loss, might be dying from hypoxia; and that hypoxia-induced CNS death may not require the proapoptotic function of Abl. The Type 1 embryos, in which CNS apoptosis is abrogate by *Abl* loss, may be dying from metabolic stress that requires the proapoptotic function of Abl.

In the *Rb*-null genetic background, the proapoptotic activity of *Abl* may be enhanced owing to the loss of RB control of the nuclear Abl kinase activity. With cultured fibroblasts derived from the $Rb^{-/-}Abl^{-/-}$ embryos, a reduced apoptotic response to TNF-α has previously been reported (Chau *et al*., 2004). Whether TNF contributes to the ectopic apoptosis in the CNS or the liver of *Rb*-null embryos is presently unknown but worthy of further investigation. An unexpected result from this study was the comparable protection from apoptosis by the loss of either one or two alleles of *Abl*. This finding suggests the proapoptotic function of *Abl* to exhibit haploid insufficiency such that both alleles of *Abl* are required to support the excessive apoptosis in the CNS and the liver of *Rb*-null embryos. This gene dosage effect on the proapoptotic function suggests that a high level of Abl protein, in addition to its tyrosine kinase, is required for the activation of apoptosis. Previous studies have suggested Abl to bind p53 and p73 and to associate with the RB–E2F complex (Welch and Wang, 1993,

Table 1 Phenotype summary of $Rb^{-/-}$ mouse strains

Genotype	*Ectopic S-phase (CNS)*	*Apoptosis in CNS*	*Apoptosis in PNS*	*Apoptosis in liver*	*Erythrocyte maturation*	References
$Rb^{-/-}$	+	+	+	+	Defective	Clarke *et al*., (1992); Jacks *et al*., (1992); Lee *et al*., (1992); Zacksenhaus *et al*., (1996)
$Rb^{-/-}$ *E2F1*$^{-/-}$	–	–	+	ND	Partially defective	Tsai *et al*., (1998)
$Rb^{-/-}$ *p53*$^{-/-}$	+	–	+	ND	ND	Macleod *et al*., (1996)
$Rb^{-/-}$ *Apaf-1*$^{-/-}$	+	–	+/–	ND	Defective	Guo *et al*., (2001)
$Rb^{-/-}$ *caspase 3*$^{-/-}$	ND	+	–	+	Defective	Simpson *et al*., (2001)
$Rb^{-/-}$ *E2F3*$^{+/-}$	+; –	–	+/–	ND	ND	Ziebold *et al*., (2001)
$Rb^{-/-}$ *E2F3*$^{-/-}$	–	–	+/–	–	Partially defective	Ziebold *et al*., (2001)
$Rb^{-/-}$ *Id2*$^{-/-}$	–	–	–	ND	Normal	Lasorella *et al*., (2000)
$Rb^{-/-}$ *Arf*$^{-/-}$	+	+	+	ND	ND	Tsai *et al*., (2002)
$Rb^{-/-}$ *with* $Rb^{+/+}$ *placenta*	+	–	–	–	Almost normal	de Bruin *et al*., (2003); Wu *et al*., (2003)
$Rb^{-/-}$ *Abl*$^{+/-}$; $Rb^{-/-}$ *Abl*$^{-/-}$	+	+; – (E11.5–12.5) + (E13.5)	+	–	Defective	This report

Abbreviations: Rb, retinoblastoma; CNS, central nervous system; PNS, peripheral nervous system; ND, not determined; +, defect in all embryos; –, defect rescued in all embryos; +/–, defect partially rescued in all embryos; +; –, defect rescued in a percentage of the embryos examined.

1995; Goga *et al*., 1995; Agami *et al*., 1999; Gong *et al*., 1999; Yuan *et al*., 1999; Goldberg *et al*., 2002). In the context of these protein–protein interactions, Abl is shown to stimulate transcription and may thus contribute to p53/p73 and/or E2F-dependent activation of apoptosis (Welch and Wang, 1993, 1995; Goga *et al*., 1995; Agami *et al*., 1999; Gong *et al*., 1999; Yuan *et al*., 1999; Goldberg *et al*., 2002). A reduction of Abl protein level caused by the loss of one *Abl* allele may decrease the formation of these proapoptotic transcription complexes, and thus compromise *Abl*-dependent apoptosis in the *Rb*-null embryos.

The $Abl^{+/-}$ mice are healthy and normal; hence, one allele of *Abl* is sufficient for the proper development of the mouse (Tybulewicz *et al*., 1991; Li *et al*., 2000). It thus appears that the gene dosage-dependent proapoptotic function of *Abl*, manifested in the *Rb*-null embryos, is dispensable for normal embryonic development. In the $Abl^{+/-}$ genetic background, protection from apoptosis is correlated with prolonged survival of the *Rb*-null embryos. However, reduced apoptosis did not result in prolonged survival in the $Rb^{-/-}Abl^{-/-}$ embryos. The $Abl^{-/-}$ mice exhibit a variety of developmental defects leading to late embryonic or neonatal lethality (Tybulewicz *et al*., 1991; Li *et al*., 2000). The Abl protein is localized to the cytoplasm and the nucleus and undergoes nucleo-cytoplasmic shuttling (Wang, 2000; Woodring *et al*., 2003). The cytoplasmic Abl is activated by growth factors and cell adhesion to regulate F-actin dynamics (Woodring *et al*., 2003). The cytoplasmic functions of Abl are not likely to be regulated by RB; thus, the developmental defects of $Abl^{-/-}$ mice may be owing to defects other than the disruption of ABL/RB interaction. That the $Rb^{-/-}Abl^{-/-}$ embryos did not gain a survival advantage may therefore be explained by the additional developmental defects caused by the homozygous knockout of *Abl*.

In previous studies, we have found that the knockout of *Abl* does not affect IR-induced apoptosis in the developing retina of newborn mice (Borges *et al*., 2004). However, explanted *Abl*-null thymocytes exhibit reduced apoptotic response to TNF-α (Chau *et al*., 2004) and to IR in *ex vivo* cultures (LD Wood and JYJ Wang unpublished). Others have reported that Abl enhances IR-induced apoptosis in several human cancer cell lines (Yuan *et al*., 1997, 1999; Agami *et al*., 1999; Takao *et al*., 2000). Our findings of tissue-specific and developmental stage-dependent role of *Abl* in the apoptosis of *Rb*-null embryos, together with previously published results, suggest that the proapoptotic function of Abl is modulated by the cell context as well as the nature of the death stimuli. Nevertheless, this study provides *in vivo* evidence to support the proapoptotic function of Abl.

Materials and methods

Mice embryos

$Rb^{+/-}Abl^{+/-}$ mice were then inter-crossed to generate embryos for this study (129S6/SvEvTac background). Genotyping was performed as previously described (Tybulewicz *et al*., 1991; Jacks *et al*., 1992). Timed-pregnant females, detected by vaginal plugs (E0.5), were killed and embryos were removed between embryonic days 10.0 and 14.5 (E10.5–E14.5). From the embryos collected, tail DNA was extracted for genotyping and blood smear slides were performed. Blood smear slides were fixed and stained with Wright-Giemsa, according to the manufacturer's instructions (Fisher). Both the viable and the dead embryos were genotyped, whereas only viable embryos were fixed with 10% phosphate-buffered formalin, embedded in paraffin, sagitally sectioned and stained. In some experiments, an intraperitoneal injection (60 mg/kg body mass) of BrdU was given to the pregnant female mice 1 h before the collection of the embryos. The Animal Care and Use Committee of UCSD approved the animal protocols used in this study.

Statistical analysis

Statistical analysis was performed using Prism 4, 2003, from GraphPad Software, Inc. We used paired, unpaired *t*-test or one-way analyses of variance (ANOVA) (Dunnett's multiple comparison test) to analyse the results. The histograms display the mean and standard error (s.e.m.).

Immunohistochemistry (IHC) and TUNEL assay

Deparaffinized sections were immunostaining with anti-PCNA, (Calbiochem, San Diego, CA, USA), or anti-BrdU (Amersham Biosciences, Pittsburgh, PA, USA) and reveled with anti-mouse Alexa-555 (Promega Corporation, Madison, WI, USA). The tissue sections were then counterstained with 10 μg/ml Hoechst-33258 (Sigma-Aldrich, St Louis, MO, USA). As controls, the primary antibody was omitted from the IHC reactions. TUNEL was performed according to the manufacturer's protocol (Roche Diagnostics Corporation, Indianapolis, IN, USA).

Quantification of TUNEL-positive or BrdU-positive nuclei, and PCNA-positive cells were performed in three to five fields under the microscope ($\times 630$ of magnification) in the intermediate zone (the differentiation field) of the hindbrain (CNS) at the fourth ventricle and in the DRG. TUNEL-positive nuclei quantification in liver was performed in three to five fields per embryo under the microscope at $\times 400$ magnification. Quantification was carried out in two to five nonconsecutive sagittal sections from each embryo to decrease the possibility of regional variability. Histograms show the average number of nuclei with the indicated marker (PCNA, BrdU, TUNEL) per mm^2 plus standard error from three to seven embryos. One hundred fifty-four embryos were evaluated by the standard hematoxylin and eosin (H&E) staining to assess viability, tissue structures and to evaluate the presence of pyknotic nuclei. The number of embryos examined by H&E according to genotypes are as follows: $Rb^{+/+}Abl^{+/+}$ ($n=40$), $Rb^{-/-}Abl^{+/+}$ ($n=27$), $Rb^{-/-}Abl^{+/-}$ ($n=53$), $Rb^{-/-}Abl^{-/-}$ ($n=22$), $Rb^{+/+}Abl^{-/-}$ ($n=11$), $Rb^{+/-}$ $Abl^{+/-}$ ($n=1$). The number of embryos examined by TUNEL according to genotypes are as follows: $Rb^{+/+}Abl^{+/+}$($n=14$), $Rb^{-/-}Abl^{+/+}$ ($n=19$), $Rb^{-/-}Abl^{+/-}$ ($n=19$), $Rb^{-/-}Abl^{-/-}$ ($n=20$), $Rb^{+/+}Abl^{-/-}$ ($n=11$), $Rb^{+/-}$ $Abl^{+/-}$ ($n=1$). Thus, a total of 84 embryos were processed for TUNEL assays. Embryos that showed high incidence of cell death by H&E staining (presence of pyknotic nuclei) also showed high incidence of TUNEL$^+$ nuclei.

Acknowledgements

We thank Rimma Levenzon for technical support. HLB is supported by CNPq (Brazil). This study was funded by a grant from the National Institutes of Health, USA to JYJW (CA58320).

References

Adams PD, Li X, Sellers WR, Baker KB, Leng X, Harper JW *et al*. (1999). Retinoblastoma protein contains a C-terminal motif that targets it for phosphorylation by cyclin–cdk complexes. *Mol Cell Biol* **19**: 1068–1080.

Agami R, Blandino G, Oren M, Shaul Y. (1999). Interaction of c-Abl and p73alpha and their collaboration to induce apoptosis. *Nature* **399**: 809–813.

Aloisi A, Di Gregorio S, Stagno F, Guglielmo P, Mannino F, Sormani MP *et al*. (2006). BCR-ABL nuclear entrapment kills human CML cells: *ex vivo* study on 35 patients with the combination of imatinib mesylate and leptomycin B. *Blood* **107**: 1591–1598.

Alvarez AR, Sandoval PC, Leal NR, Castro PU, Kosik KS. (2004). Activation of the neuronal c-Abl tyrosine kinase by amyloid-beta-peptide and reactive oxygen species. *Neurobiol Dis* **17**: 326–336.

Borges HL, Chao C, Xu Y, Linden R, Wang JY. (2004). Radiation-induced apoptosis in developing mouse retina exhibits dose-dependent requirement for ATM phosphorylation of p53. *Cell Death Differ* **11**: 494–502.

Chau BN, Chen TT, Wan YY, DeGregori J, Wang JY. (2004). Tumor necrosis factor alpha-induced apoptosis requires p73 and c-ABL activation downstream of RB degradation. *Mol Cell Biol* **24**: 4438–4447.

Chau BN, Wang JY. (2003). Coordinated regulation of life and death by RB. *Nat Rev Cancer* **3**: 130–138.

Clarke AR, Maandag ER, van Roon M, van der Lugt NM, van der Valk M, Hooper ML *et al*. (1992). Requirement for a functional Rb-1 gene in murine development. *Nature* **359**: 328–330.

Darnell GA, Antalis TM, Johnstone RW, Stringer BW, Ogbourne SM, Harrich D *et al*. (2003). Inhibition of retinoblastoma protein degradation by interaction with the serpin plasminogen activator inhibitor 2 via a novel consensus motif. *Mol Cell Biol* **23**: 6520–6532.

de Bruin A, Wu L, Saavedra HI, Wilson P, Yang Y, Rosol TJ *et al*. (2003). Rb function in extraembryonic lineages suppresses apoptosis in the CNS of Rb-deficient mice. *Proc Natl Acad Sci USA* **100**: 6546–6551.

Goga A, Liu X, Hambuch TM, Senechal K, Major E, Berk AJ *et al*. (1995). p53 dependent growth suppression by the c-Abl nuclear tyrosine kinase. *Oncogene* **11**: 791–799.

Goldberg Z, Vogt Sionov R, Berger M, Zwang Y, Perets R, Van Etten RA *et al*. (2002). Tyrosine phosphorylation of Mdm2 by c-Abl: implications for p53 regulation. *EMBO J* **21**: 3715–3727.

Gong JG, Costanzo A, Yang HQ, Melino G, Kaelin Jr WG, Levrero M *et al*. (1999). The tyrosine kinase c-Abl regulates p73 in apoptotic response to cisplatin-induced DNA damage. *Nature* **399**: 806–809.

Guo Z, Yikang S, Yoshida H, Mak TW, Zacksenhaus E. (2001). Inactivation of the retinoblastoma tumor suppressor induces apoptosis protease-activating factor-1 dependent and independent apoptotic pathways during embryogenesis. *Cancer Res* **61**: 8395–8400.

Hickman ES, Moroni MC, Helin K. (2002). The role of p53 and pRB in apoptosis and cancer. *Curr Opin Genet Dev* **12**: 60–66.

Jacks T, Fazeli A, Schmitt EM, Bronson RT, Goodell MA, Weinberg RA. (1992). Effects of an Rb mutation in the mouse. *Nature* **359**: 295–300.

Kaufman MH (ed). (1992). *Atlas of Mouse Development*. Academic Press: UK.

Lasorella A, Noseda M, Beyna M, Yokota Y, Iavarone A. (2000). Id2 is a retinoblastoma protein target and mediates signalling by Myc oncoproteins. *Nature* **407**: 592–598.

Lee C, Chang JH, Lee HS, Cho Y. (2002). Structural basis for the recognition of the E2F transactivation domain by the retinoblastoma tumor suppressor. *Genes Dev* **16**: 3199–3212.

Lee EY, Chang CY, Hu N, Wang YC, Lai CC, Herrup K *et al*. (1992). Mice deficient for Rb are nonviable and show defects in neurogenesis and haematopoiesis. *Nature* **359**: 288–294.

Lee JO, Russo AA, Pavletich NP. (1998). Structure of the retinoblastoma tumour-suppressor pocket domain bound to a peptide from HPV E7. *Nature* **391**: 859–865.

Levinson NM, Kuchment O, Shen K, Young MA, Koldobskiy M, Karplus M *et al*. (2006). A Src-like inactive conformation in the abl tyrosine kinase domain. *PLoS Biol* **4**: e144.

Li B, Boast S, de los Santos K, Schieren I, Quiroz M, Teitelbaum SL *et al*. (2000). Mice deficient in Abl are osteoporotic and have defects in osteoblast maturation. *Nat Genet* **24**: 304–308.

Liu H, Dibling B, Spike B, Dirlam A, Macleod K. (2004). New roles for the RB tumor suppressor protein. *Curr Opin Genet Dev* **14**: 55–64.

Liu X, Clements A, Zhao K, Marmorstein R. (2006). Structure of the human papillomavirus E7 oncoprotein and its mechanism for inactivation of the retinoblastoma tumor suppressor. *J Biol Chem* **281**: 578–586.

Macleod KF, Hu Y, Jacks T. (1996). Loss of Rb activates both p53-dependent and independent cell death pathways in the developing mouse nervous system. *EMBO J* **15**: 6178–6188.

MacPherson D, Sage J, Crowley D, Trumpp A, Bronson RT, Jacks T. (2003). Conditional mutation of Rb causes cell cycle defects without apoptosis in the central nervous system. *Mol Cell Biol* **23**: 1044–1053.

Morgenbesser SD, Williams BO, Jacks T, DePinho RA. (1994). p53-dependent apoptosis produced by Rb-deficiency in the developing mouse lens. *Nature* **371**: 72–74.

Morris EJ, Dyson NJ. (2001). Retinoblastoma protein partners. *Adv Cancer Res* **82**: 1–54.

Nguyen DX, McCance DJ. (2005). Role of the retinoblastoma tumor suppressor protein in cellular differentiation. *J Cell Biochem* **94**: 870–879.

Rubin SM, Gall AL, Zheng N, Pavletich NP. (2005). Structure of the Rb C-terminal domain bound to E2F1-DP1: a mechanism for phosphorylation-induced E2F release. *Cell* **123**: 1093–1106.

Sherr CJ, McCormick F. (2002). The RB and p53 pathways in cancer. *Cancer Cell* **2**: 103–112.

Simpson MT, MacLaurin JG, Xu D, Ferguson KL, Vanderluit JL, Davoli MA *et al*. (2001). Caspase 3 deficiency rescues peripheral nervous system defect in retinoblastoma nullizygous mice. *J Neurosci* **21**: 7089–7098.

Sionov RV, Moallem E, Berger M, Kazaz A, Gerlitz O, Ben-Neriah Y *et al*. (1999). c-Abl neutralizes the inhibitory effect of Mdm2 on p53. *J Biol Chem* **274**: 8371–8374.

Takao N, Mori R, Kato H, Shinohara A, Yamamoto K. (2000). c-Abl tyrosine kinase is not essential for ataxia telangiectasia mutated functions in chromosomal maintenance. *J Biol Chem* **275**: 725–728.

Tsai KY, Hu Y, Macleod KF, Crowley D, Yamasaki L, Jacks T. (1998). Mutation of E2f-1 suppresses apoptosis and inappropriate S phase entry and extends survival of Rb-deficient mouse embryos. *Mol Cell* **2**: 293–304.

Tsai KY, MacPherson D, Rubinson DA, Crowley D, Jacks T. (2002). ARF is not required for apoptosis in Rb mutant mouse embryos. *Curr Biol* **12**: 159–163.

Tybulewicz VL, Crawford CE, Jackson PK, Bronson RT, Mulligan RC. (1991). Neonatal lethality and lymphopenia in mice with a homozygous disruption of the c-abl proto-oncogene. *Cell* **65**: 1153–1163.

Vella V, Zhu J, Frasca F, Li CY, Vigneri P, Vigneri R *et al*. (2003). Exclusion of c-Abl from the nucleus restrains the p73 tumor suppression function. *J Biol Chem* **278**: 25151–25157.

Vigneri P, Wang JY. (2001). Induction of apoptosis in chronic myelogenous leukemia cells through nuclear entrapment of BCR-ABL tyrosine kinase. *Nat Med* **7**: 228–234.

Wang JY. (2000). Regulation of cell death by the Abl tyrosine kinase. *Oncogene* **19**: 5643–5650.

Welch PJ, Wang JY. (1993). A C-terminal protein-binding domain in the retinoblastoma protein regulates nuclear c-Abl tyrosine kinase in the cell cycle. *Cell* **75**: 779–790.

Welch PJ, Wang JY. (1995). Abrogation of retinoblastoma protein function by c-Abl through tyrosine kinase-dependent and -independent mechanisms. *Mol Cell Biol* **15**: 5542–5551.

Woodring PJ, Hunter T, Wang JY. (2003). Regulation of F-actin-dependent processes by the Abl family of tyrosine kinases. *J Cell Sci* **116**: 2613–2626.

Wu L, de Bruin A, Saavedra HI, Starovic M, Trimboli A, Yang Y *et al*. (2003). Extra-embryonic function of Rb is essential for embryonic development and viability. *Nature* **421**: 942–947.

Xiao B, Spencer J, Clements A, Ali-Khan N, Mittnacht S, Broceno C *et al*. (2003). Crystal structure of the retinoblastoma tumor suppressor protein bound to E2F and the molecular basis of its regulation. *Proc Natl Acad Sci USA* **100**: 2363–2368.

Yuan ZM, Huang Y, Ishiko T, Kharbanda S, Weichselbaum R, Kufe D. (1997). Regulation of DNA damage-induced apoptosis by the c-Abl tyrosine kinase. *Proc Natl Acad Sci U S A* **94**: 1437–1440.

Yuan ZM, Shioya H, Ishiko T, Sun X, Gu J, Huang YY *et al*. (1999). p73 is regulated by tyrosine kinase c-Abl in the apoptotic response to DNA damage. *Nature* **399**: 814–817.

Zacksenhaus E, Jiang Z, Chung D, Marth JD, Phillips RA, Gallie BL. (1996). pRb controls proliferation, differentiation, and death of skeletal muscle cells and other lineages during embryogenesis. *Genes Dev* **10**: 3051–3064.

Ziebold U, Reza T, Caron A, Lees JA. (2001). E2F3 contributes both to the inappropriate proliferation and to the apoptosis arising in Rb mutant embryos. *Genes Dev* **15**: 386–391.